OPTICA

Ultrafast temporal phase-resolved nonlinear optical spectroscopy in the molecular frame

Siddhant Pandey,[1] Liang Z. Tan,[2] Francis Walz,[1] Varun Makhija,[3] and Niranjan Shivaram[1,4,*]

[1]Department of Physics and Astronomy, Purdue University, West Lafayette, Indiana 47907, USA
[2]Molecular Foundry, Lawrence Berkeley National Laboratory, Berkeley, California 94720, USA
[3]Department of Chemistry and Physics, University of Mary Washington, Fredericksburg, Virginia 2240, USA
[4]Purdue Quantum Science and Engineering Institute, Purdue University, West Lafayette, Indiana 47907, USA
*niranjan@purdue.edu

Received 19 December 2023; revised 29 April 2024; accepted 3 May 2024; published 30 May 2024

In an ultrafast nonlinear optical interaction, the electric field of the emitted nonlinear signal provides direct access to the induced nonlinear transient polarization or transient currents and thus carries signatures of ultrafast dynamics in a medium. Measurement of the electric field of such signals offers sensitive observables to track ultrafast electron dynamics in various systems. In this work, we resolve the real-time phase of the electric field of a femtosecond third-order nonlinear optical signal in the molecular frame. The electric field emitted from impulsively pre-aligned gas-phase molecules at room temperature, in a degenerate four-wave mixing scheme, is measured using a spectral interferometry technique. The nonlinear signal is measured around a rotational revival to extract its molecular-frame angle dependence from pump-probe time-delay scans. By comparing these measurements for two linear molecules, carbon dioxide and nitrogen, we show that the measured second-order phase parameter (temporal chirp) of the signal is sensitive to the valence electronic symmetry of the molecules, whereas the amplitude of the signal does not show such sensitivity. We compare measurements to theoretical calculations of the chirp observable in the molecular frame. This work is an important step towards using electric field measurements in nonlinear optical spectroscopy to study ultrafast dynamics of electronically excited molecules in the molecular frame.

https://doi.org/10.1364/OPTICA.515959

1. INTRODUCTION

Ultrafast dynamics in molecules occur on time scales ranging from attoseconds to picoseconds. These dynamics are routinely studied using photoionization based spectroscopies, ultrafast electron diffraction, and all-optical spectroscopies [1–4]. Due to the multidimensional nature of the problem, the study of ultrafast dynamics in molecules typically requires a number of complementary measurements to disentangle the dynamics for any given system. An all-optical experimental observable that is sensitive to electronic symmetry could offer important insight into ultrafast electron and electron-nuclear dynamics. Ultrafast optical measurements, including transient absorption spectroscopy, rely on the nonlinear optical response of the target molecule. In symmetric top molecules, the two unique components of the polarizability tensor, $\alpha_{\parallel}$ and $\alpha_{\perp}$, contain limited information compared to the multiple nonzero tensor components of higher-order hyperpolarizability tensors. A measurement that probes the higher-order nonlinear response of molecules can thus provide detailed information on the symmetry of involved electronic states. Further, in an all-optical measurement, completely resolving the emitted electric field (E-field) provides direct access to the induced polarization, which is intricately related to the ultrafast evolution of the system being studied. Combining ultrafast field-resolved spectroscopy with nonlinear optical response measurements will thus enable tracking of transient electronic symmetries in excited molecules. Recently, ultrafast electric field measurements using attosecond streaking [5–7], direct field sampling [8–16], and spectral interferometry [17] have emerged as sensitive methods to probe ultrafast dynamics. Applying field-resolved nonlinear optical spectroscopy to laser excited molecules is an important step towards realizing the full potential of nonlinear optical spectroscopy in probing ultrafast dynamics.

Due to inversion symmetry, typically, the first non-vanishing nonlinear response in gas-phase molecules is the third-order response, corresponding to molecular second hyperpolarizabilities. In this work, we measure the molecular frame third-order response in gas-phase linear molecules at room temperature, by directly measuring the full nonlinear E-field emitted during degenerate four-wave mixing (DFWM) [18] in pre-aligned molecules. This nonlinearity has three dominant sources: bound electronic, plasma, and rotational nonlinearity [19]. Vibrational nonlinearities are not observed due to the limited bandwidth of our laser pulses. Rotational nonlinearity, which arises from nuclear motion,

is slower compared to the near-instantaneous electronic nonlinearity, which arises from the distortion of the molecular electron cloud due to the laser's electric field [20]. For low enough laser intensities, the plasma nonlinearity can be ignored. When all the DFWM laser pulses have polarization along a fixed axis in the lab frame, say z, the emitted third-order signal in the frequency domain from a single molecule can be written as

$$E_{\text{signal},z}(\omega,\theta) = i\chi^{(3)}_{zzzz}(\omega,\theta)E_{1,z}(\omega)E^{*}_{2,z}(\omega)E_{3,z}(\omega), \quad (1)$$

where θ is the relative angle between the laser polarization along $\hat{z}$ and the molecules' symmetry-axis; ω is the angular frequency; and the subscripts 1, 2, and 3 correspond to the three DFWM pulses, which are assumed to be temporally overlapped with zero time delay. For linear molecules, which will be the focus of this work, the lab-frame third-order susceptibility can be related to the molecular frame second hyperpolarizabilities as

$$\chi^{(3)}_{zzzz}(\omega,\theta) = \gamma^{(2)}_{zzzz}(\omega)\cos^4(\theta) + \frac{3}{2}\gamma^{(2)}_{zxxx}(\omega)\sin^2(2\theta) + \gamma^{(2)}_{xxxx}(\omega)\sin^4(\theta). \quad (2)$$

It is well known that molecules can be excited rotationally with intense non-resonant laser pulses, leading to periodic rotational revivals on the time scale of tens of picoseconds [21–24]. Electron dynamics, on the other hand, occur on femtosecond and attosecond time scales after interaction with the excitation laser pulse. This separation of time scales allows probing of femtosecond electronic response using DFWM at rotational revivals by first exciting a rotational wavepacket. Once the DFWM input pulses are characterized, a measurement of $E_{\text{signal}}(t)$ from a rotational wavepacket can give direct access to molecular frame second hyperpolarizability. This is essentially similar to measuring the lab-frame nonlinear response in Eq. (2) for multiple θ to obtain the molecular frame response tensor components.

2. EXPERIMENTAL METHOD

In our temporal phase-resolved alignment pump-DFWM experiment (see Fig. 1), 60 fs near-infrared (IR) pulses centered around 800 nm are first split and delayed. One arm forms the alignment pump beam, and the other is split again into three weaker DFWM probe beams using a mask, in the folded BOXCARS geometry [18]. One of the DFWM probe beams is further split to derive a reference pulse. The alignment pump excites a rotational wavepacket, which is then probed using the DFWM beams. All four pulses intersect inside a gas cell containing the target gas at room temperature and a pressure of 4 bar, in a non-collinear geometry. The intensity of the pump pulse was estimated from the fitting procedure to be 8 TW/cm^2, while the average intensity of the probe pulses is estimated to be <4 TW/cm^2. The crossing angles are small enough such that time-smearing is small in comparison to the pulse duration. The time delay (T) between the alignment pump and probe pulses is varied using an optical delay stage. The pump and the probe beams are co-polarized. In the folded BOXCARS geometry, the emitted nonlinear signal propagates along a separate direction and is spatially isolated from all other beams using a beam-stop [18]. The emitted signal is passed through a polarizer to remove any ellipticity and coupled into a home-built spectrometer, along with the reference pulse, for spectral interferometry [25]. In our measurements, the DFWM

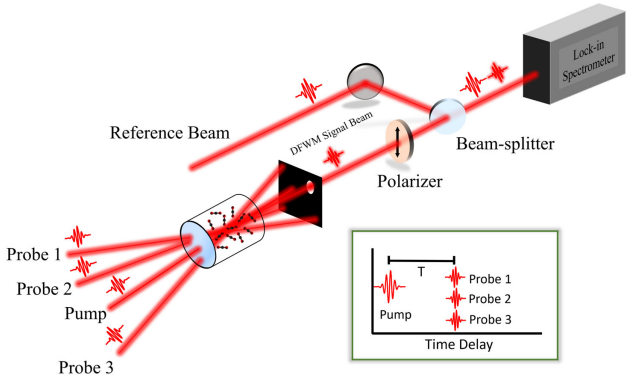

Fig. 1. Schematic of the experimental setup. The alignment pump and the time-delayed DFWM probe beams are focused into a gas cell containing the target gas at room temperature and a pressure of 4 bar. The emitted nonlinear signal is spatially isolated, cleaned with a polarizer, and combined with the external reference in a lock-in detection enabled spectrometer. The reference is separately characterized using a frequency resolved optical gating (FROG) setup (not shown).

signal from aligned molecules is ∼1% of the signal from unaligned molecules. Since both of these travel along the same phase-matched direction, it becomes essential to remove this background signal from unaligned molecules. We adapt a lock-in amplification scheme in our spectrometer to separate the weak signal from the strong background. The details of this lock-in enabled interferometry scheme will be discussed in a future publication. The use of a lock-in spectrometer results in a significant improvement of the signal-to-noise ratio (SNR) and automatic subtraction of the background nonlinear signal from unaligned molecules.

For each pump-probe time delay (T), the measured E-field phase is fit to a fifth-order polynomial in pulse time (t):

$$\varphi(t,T) = a_0(T) + a_1(T)\cdot t + a_2(T)\cdot t^2 + a_3(T)\cdot t^3 \ldots, \quad (3)$$

similar to Ref. [17]. The second-order polynomial coefficient a_2 (also known as chirp), which is the dominant nonlinear fit coefficient, is extracted as a function of the pump-probe time delay (T). Experiments that measure the absolute phase shift of a weak probe passing through pumped media often measure the zeroth-order coefficient $a_0(T)$ in this expansion [20,26]. Pump-probe studies in gases have previously measured the time-delay-dependent frequency shifts [27], which correspond to the time-dependent refractive index and the linear coefficient $a_1(T)$. Four-wave mixing experiments in liquids have also measured the full amplitude and phase of the signal [28,29]. Such a complete measurement of the emitted E-field phase gives access to both the absolute phase shift and other higher-order terms, especially chirp [17], which is used as the main observable in our study involving gas-phase molecules.

3. RESULTS AND DISCUSSION

Previous studies have shown that by measuring the photoionization or high-harmonic generation (HHG) yield from a molecular wavepacket as a function of alignment pump-probe time delay, the yield can be retrieved as a function of the relative angle between the pump pulse polarization and the symmetry-axis of the molecule [30–36]. This deconvolution method can improve angular resolution when working with molecular ensembles having low degree of alignment, as in our experiment where $\langle\cos^2(\theta)\rangle \sim 0.35$. We perform such an analysis to retrieve the alignment angle dependence

of the nonlinear signal E-field chirp from time-delay-dependent measurements. We assume that the chirp of the emitted nonlinear signal is a function of the molecular alignment angle θ. For linear molecules interacting with a one-color pulse, inversion symmetry implies $\theta \equiv \pi - \theta$, so we can expand the angle-dependent chirp $a_2(\theta)$ in Legendre polynomials as

$$a_2(\theta) = \sum_l c_l P_l(\cos(\theta)) \tag{4}$$

with even values of l. Upon taking the expectation value of this equation with the pump-excited rotational wavepacket, the left-hand side becomes the experimentally measured chirp

$$a_2(T) = \sum_j c_j \langle P_j \rangle (T). \tag{5}$$

Using a suitable set of pulse parameters for the alignment pump, we simulate the time evolution of the excited rotational wavepacket and calculate the expectation value of the Legendre polynomials on the right-hand side of Eq. (5), which can then be inverted to find the expansion coefficients c_j (see Refs. [31,32] for more details). The rotational temperature of the gas is the same as its thermal temperature (295 K), and the pump pulse duration is measured to be 60 fs using a commercial second-harmonic generation (SHG) based frequency resolved optical gating (FROG) device. In the fitting procedure, the intensity of the pump pulse in the focal region was allowed to vary within reasonable bounds, from 5 to 40 TW/cm^2. To account for collisional dephasing of the excited rotational wavepacket, we also include a single-exponential decay parameter in the fitting procedure [37]. The measured signal E-field phase, as a function of pulse time (t) and pump-probe time delay (T), is shown in Fig. 2(a) for N_2 molecules and in Fig. 2(b) for CO_2 molecules, as contour plots. Figure 2(c) shows a representative plot of the pulse time (t) dependent amplitude and phase of the nonlinear signal for a fixed time delay (T). The phase is fit to a polynomial [Eq. (3)] using an amplitude weighted fit from which the chirp is extracted as a function of T. Figure 2(d) shows the extracted chirp as a function of T for both N_2 and CO_2 molecules. The alignment angle-dependent chirp in the molecular frame is retrieved by using a fitting and inversion procedure that provides coefficients c_j, as described above. Figure 3(a) shows the molecular-frame chirp of the nonlinear optical signal for N_2 and CO_2 molecules. These experimental chirp plots show distinct angular dependence of the chirp for the two molecules, which have different ground state electronic symmetries. The corresponding highest occupied molecular orbital (HOMO) for the two molecules is shown in

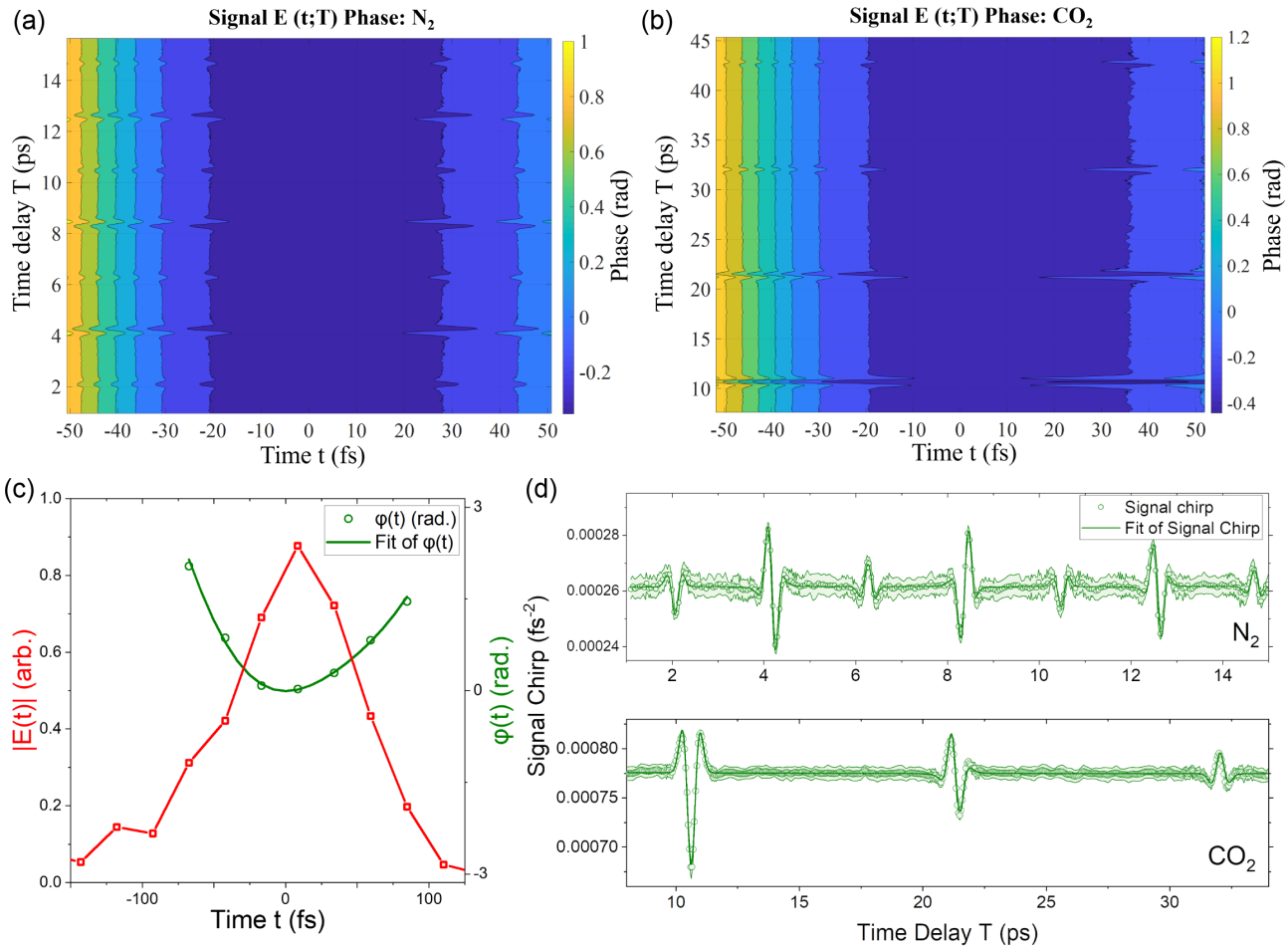

Fig. 2. (a) Temporal phase of the nonlinear signal E-field from pre-aligned N_2 molecules and (b) from pre-aligned CO_2 molecules, as a function of pulse time (t) and time delay (T). (c) Representative plot of E-field amplitude and phase along with a polynomial fit of the phase. The temporal resolution of the field measurement from spectral interferometry is 28 fs. (d) For each pump-probe time delay T, the measured E-field phase is fit with a polynomial in pulse time t. The second-order fit coefficient (chirp) is plotted as a function of T for N_2 and CO_2. The error band represents standard error. The chirp of the input probe pulses is 0.00017 fs^{-2}.

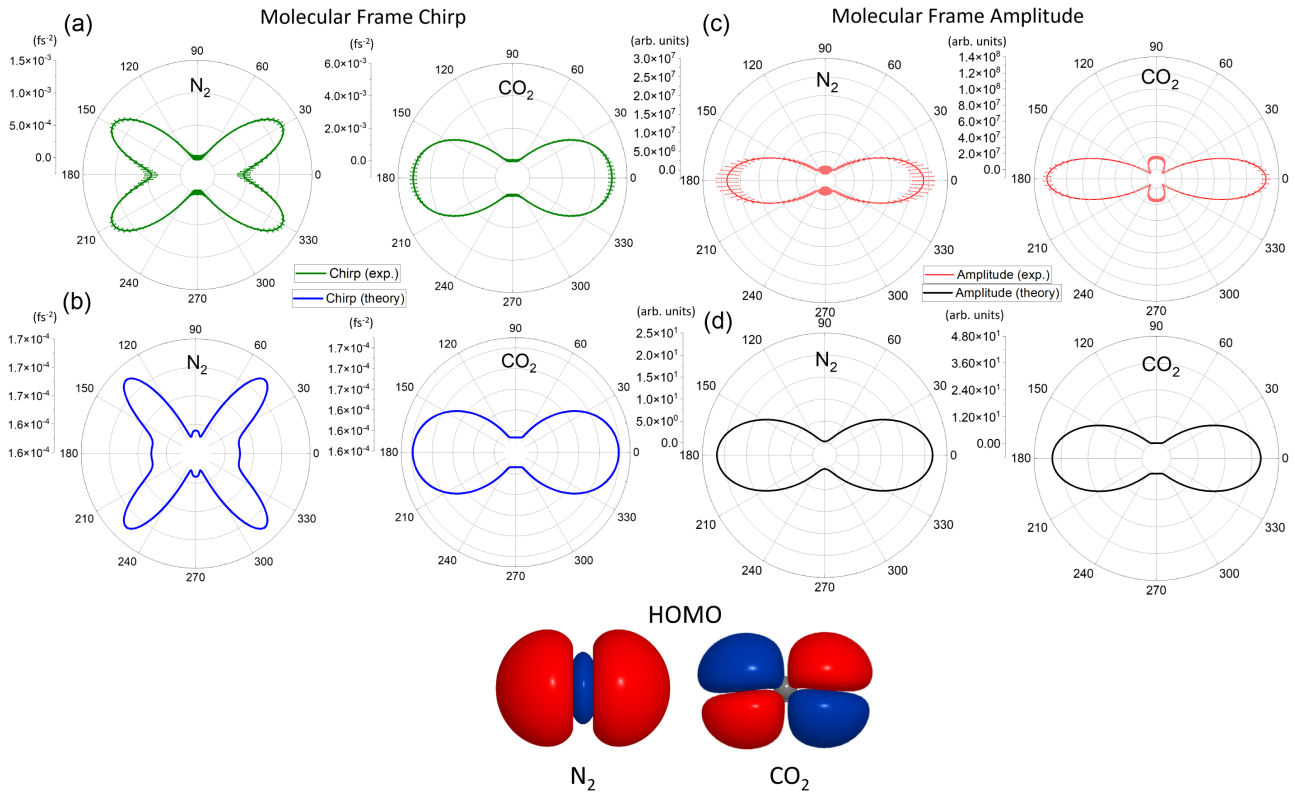

Fig. 3. (a) Alignment angle-dependent molecular-frame nonlinear signal E-field chirp retrieved from the experimental data, for N_2 and CO_2. (b) Theoretical calculations of the alignment angle-dependent E-field chirp for N_2 and CO_2. (c) Alignment angle-dependent molecular-frame E-field amplitude (pulse time-integrated). (d) Same as (c) from theoretical calculations. Highest occupied molecular orbitals (HOMO) for N_2 and CO_2 molecules, showing their distinct σ and π bonding character, respectively, are shown in the bottom panel for reference. While the molecular frame chirp does not directly correspond to the shape of the HOMOs, the chirp is seen to be distinctly different for the two molecules.

the bottom panel of Fig. 3. To investigate the origin of the angle-dependent chirp, the nonlinear electronic response of N_2 and CO_2 molecules was calculated using the DFWM pulse sequence used in the experiment. From the calculated signal E-fields, the phase was fit similar to the experimental data to obtain the calculated molecular-frame angle-dependent chirp for a single molecule. The details of the calculation are provided in the next section. The chirp of the calculated signal field, as shown in Fig. 3(b), shows good agreement with the experimentally determined angle-dependent chirp [Fig. 3(a)], with minor deviations in the maximal angle likely arising from the coupled-cluster electronic structure methodology (Section 4). These calculations support the interpretation that the angle dependence of the signal chirp observed in our experiment is electronic in origin and that propagation effects of the weak nonlinear signal in the dense target medium are negligible. The low-intensity, non-resonant probe pulses used in this experiment interact perturbatively with the target molecules, and the signal predominantly originates from valence electrons. The angular dependence of molecular-frame chirp of the nonlinear signals from N_2 and CO_2 is thus sensitive to the differences in their valence electronic character. Multiple previous studies have measured and calculated the angular dependence of photoionization signals [38–42], or emission of HHG light [43–45] in aligned molecules. Establishing direct correspondence between the measured angular distribution and the HOMO wavefunction is non-trivial in these studies though molecular orbital tomography has been successful in some cases [46,47]. In our measurement, we observe the sensitivity of the molecular-frame chirp to differences in electronic symmetry in a perturbative all-optical probing scheme, even though a direct correspondence to the shape of the HOMO for the two molecules is not seen.

We perform a similar analysis to retrieve the alignment angle dependence of the (pulse time-integrated) amplitude of the emitted signal E-field. Figure 3(c) shows that the amplitude of the measured signal is not sensitive to electronic character differences between the two molecules. The corresponding single-molecule theoretical calculations of the amplitude agree well with the experimental data. This demonstrates that electric field measurement in nonlinear spectroscopy offers new observables such as the chirp that are sensitive to the electronic character and offer information beyond measurement of the intensity of the signal. Below, we briefly provide an explanation for the difference in sensitivity to electronic symmetries for the chirp and amplitude observables.

In linear molecules, the magnitude of $\gamma^{(2)}_{zzzz}$ is generally larger than any other component of the second-hyperpolarizability tensor, and, therefore (see Supplement 1 for details), the amplitude and phase of the probed third-order nonlinear response in the frequency domain may be approximated using Eq. (2) as (frequency dependence is not shown)

$$|\chi^{(3)}_{zzzz}(\theta)| \approx |\gamma^{(2)}_{zzzz}| \cos^4(\theta), \tag{6}$$

$$\varphi(\theta) \approx \varphi_{zzzz} + 6\left|\frac{\gamma^{(2)}_{zzxx}}{\gamma^{(2)}_{zzzz}}\right| \varphi_{zzxx} \tan^2(\theta) + \left|\frac{\gamma^{(2)}_{xxxx}}{\gamma^{(2)}_{zzzz}}\right| \varphi_{xxxx} \tan^4(\theta). \tag{7}$$

It is seen from Eqs. (6) and (7) that the magnitude of the frequency-domain lab-frame nonlinear response, which is proportional to the amplitude of the measured nonlinear signal, contains only the predominant second-hyperpolarizability ($\gamma^{(2)}$) tensor component. Meanwhile, the frequency-dependent phase, which is required to obtain the time-dependent phase (and hence chirp), contains additional terms with multiple tensor components of $\gamma^{(2)}$. This provides a possible explanation for the sensitivity of the molecular-frame nonlinear signal chirp to the valence electronic character while the amplitude shows the same angular behavior for the two linear molecules. Although the amplitude of this nonlinear optical response is well understood, more work is needed to better understand the origins of the phase of these tensor components and their relation to electronic symmetries.

4. CALCULATION DETAILS

Electronic structure models of CO_2 and N_2 molecules were constructed using the coupled-cluster singles and doubles (CCSD) method, with the 6-31 G(d,p) Gaussian basis set, and solved using the Dalton software [48]. These models were constructed by selecting "bright" states, which have finite transition dipole moments to the ground state, and energetically low-lying states, which have finite transition dipole to those bright states. All the bright states in these models have B_u symmetry. More details are given in Supplement 1.

We performed theoretical calculations of the emitted signal E-field using Lindblad equation simulations in the time domain, solving

$$\dot{\rho}(t) = -\frac{i}{\hbar}[H(t), \rho(t)] + \mathcal{L}_D\rho(t) \tag{8}$$

with the Hamiltonian

$$H(\vec{r}, t) = \Omega + \vec{\mu} \cdot (\vec{E}_1(\vec{r}, t) + \vec{E}_2(\vec{r}, t) + \vec{E}_3(\vec{r}, t)). \tag{9}$$

In these simulations, we use DFWM pulses $\vec{E}_1(\vec{r}, t)$, $\vec{E}_2(\vec{r}, t)$, and $\vec{E}_3(\vec{r}, t)$ with frequencies, durations, intensities, chirp, and polarizations that are the same as the experiment. The alignment pump is not included in the simulations as its only purpose was to align the molecules; alignment effects were captured in the simulations by rotating the DFWM pulses in the molecular frame. Excited state energy levels Ω and transition dipole moments $\vec{\mu}$ are obtained from CCSD calculations. We included population relaxation and dephasing times of 1 ps in the Lindbladian $\mathcal{L}_D$; however, the results were insensitive to these values as the signal is nonzero only during the duration of pulse overlap, which is much shorter than the dephasing and relaxation times. The Lindblad equation was numerically solved using the Euler method with fixed time step of 0.1 fs, using the UTPS simulation package [49].

The result of solving Eq. (8) is the time-domain polarization $\vec{P}(\vec{r}, t) = \mathrm{Tr}[\vec{\mu}\rho(\vec{r}, t)]$. To extract the third-order nonlinear signal electric field, we impose phase-matching conditions by selecting only wavevectors parallel to the signal propagation direction

$$\vec{P}_{\mathrm{sig}}(t) = \int \mathrm{d}^3 r e^{-i\vec{k}\cdot\vec{r}}\vec{P}(\vec{r}, t) \tag{10}$$

with $\vec{k} = \vec{k}_1 - \vec{k}_2 + \vec{k}_3$ being the signal wavevector corresponding to the phase-matching conditions of Eq. (1). These calculations were repeated for 100 alignment angles of the molecules between 0° and 180°. The signal amplitude and chirp from these simulations were fit using the same methodology described above for the experimental data.

5. CONCLUSION

Field-resolved ultrafast spectroscopy is emerging as a sensitive approach to measure ultrafast dynamics on femtosecond and subfemtosecond time scales in various systems. While recent studies have used field-resolved ultrafast measurement in solids [16] and liquids [50], to our knowledge, no previous work has demonstrated temporal phase-resolved perturbative nonlinear spectroscopy in laser excited pre-aligned molecules in the gas phase. In this work, we have shown that the angle dependence of the measured E-field chirp corresponding to the perturbative electronic nonlinear response in molecules can act as a probe of changes in their valence electronic symmetry, even though a direct correspondence to the shape of the HOMO is not observed. By comparing the angle dependence of the measured E-field chirp and amplitude, we have found that the phase of the emitted nonlinear E-field can be more sensitive than the amplitude of the emitted signal to the electronic symmetry of molecules. Further, we have demonstrated sensitivity of the nonlinear E-field chirp to the electronic character in molecules with poor degree of alignment ($\langle\cos^2(\theta)\rangle \sim 0.35$) at room temperature, in a perturbative interaction not involving ionization, which has not been previously possible. Our experimental data are well-supported by theoretical calculations on the single molecule nonlinear response. A more detailed mechanistic understanding of the heightened sensitivity of E-field chirp to electronic nonlinearities is still needed.

The experiment presented here is an important application of femtosecond electric field measurements to study electronic nonlinear response in the molecular frame. Complementary to existing approaches such as 2D electronic spectroscopy, the use of the temporal phase parameters as observables can be extended to electronically excited states in atoms, molecules, and solids, thus opening the possibility to disentangle complex quantum dynamics in real time with high temporal resolution. Additionally, the sensitivity of the E-field phase to differences in electronic symmetry, as demonstrated in the present work, provides a tool to study the transient changes in symmetry of electronic states in molecules as they evolve on excited potential energy surfaces. Furthermore, the demonstrated feasibility of molecular frame measurements at room temperature and high pressure in simple molecules is a first step towards such measurements in larger molecules, in an all-optical scheme without needing cooled gas jets. The ability to measure ultraweak fields with zeptojoule energies without delay scanning makes spectral interferometry [25] a suitable candidate for E-field metrology in experiments involving a low-intensity pump, such as a pulse from a HHG source, although direct field sampling has recently been demonstrated at the sub-femtojoule level [50]. In the future, measurement of field-resolved nonlinear optical signals from electronic states excited by a HHG source could offer new observables not previously accessible for the study of ultrafast dynamics.

Funding. National Science Foundation (2208061); U.S. Department of Energy (DE-AC02-05CH11231).

Acknowledgment. This material is based upon work supported by the National Science Foundation. Work at the Molecular Foundry was supported by the Office of Science, Office of Basic Energy Sciences, of the U.S. Department of

Energy. This research used resources of the National Energy Research Scientific Computing Center, a DOE Office of Science User Facility supported by the Office of Science of the U.S. Department of Energy. Publication of this article was funded in part by Purdue University Libraries Open Access Publishing Fund.

Disclosures. The authors declare no conflicts of interest.

Data availability. Data underlying the results presented in this paper are not publicly available at this time but may be obtained from the authors upon reasonable request.

Supplemental document. See Supplement 1 for supporting content.

REFERENCES

1. F. Krausz and M. Ivanov, "Attosecond physics," Rev. Mod. Phys. **81**, 163 (2009).
2. R. Geneaux, H. J. Marroux, A. Guggenmos, *et al.*, "Transient absorption spectroscopy using high harmonic generation: a review of ultrafast x-ray dynamics in molecules and solids," Philos. Trans. R. Soc. A **377**, 20170463 (2019).
3. J. Li, J. Lu, A. Chew, *et al.*, "Attosecond science based on high harmonic generation from gases and solids," Nat. Commun. **11**, 2748 (2020).
4. M. Nisoli, P. Decleva, F. Calegari, *et al.*, "Attosecond electron dynamics in molecules," Chem. Rev. **117**, 10760–10825 (2017).
5. J. Itatani, F. Quéré, G. L. Yudin, *et al.*, "Attosecond streak camera," Phys. Rev. Lett. **88**, 173903 (2002).
6. E. Goulielmakis, M. Uiberacker, R. Kienberger, *et al.*, "Direct measurement of light waves," Science **305**, 1267–1269 (2004).
7. P. Eckle, M. Smolarski, P. Schlup, *et al.*, "Attosecond angular streaking," Nat. Phys. **4**, 565–570 (2008).
8. Y. Liu, S. Gholam-Mirzaei, J. E. Beetar, *et al.*, "All-optical sampling of few-cycle infrared pulses using tunneling in a solid," Photon. Res. **9**, 929–936 (2021).
9. Y. Liu, J. E. Beetar, J. Nesper, *et al.*, "Single-shot measurement of few-cycle optical waveforms on a chip," Nat. Photonics **16**, 109–112 (2022).
10. M. R. Bionta, F. Ritzkowsky, M. Turchetti, *et al.*, "On-chip sampling of optical fields with attosecond resolution," Nat. Photonics **15**, 456–460 (2021).
11. S. B. Park, K. Kim, W. Cho, *et al.*, "Direct sampling of a light wave in air," Optica **5**, 402–408 (2018).
12. D. Hui, H. Alqattan, S. Yamada, *et al.*, "Attosecond electron motion control in dielectric," Nat. Photonics **16**, 33–37 (2022).
13. A. Schiffrin, T. Paasch-Colberg, N. Karpowicz, *et al.*, "Optical-field-induced current in dielectrics," Nature **493**, 70–74 (2013).
14. T. Paasch-Colberg, A. Schiffrin, N. Karpowicz, *et al.*, "Solid-state light-phase detector," Nat. Photonics **8**, 214–218 (2014).
15. T. Paasch-Colberg, S. Y. Kruchinin, Ö. Sağlam, *et al.*, "Sub-cycle optical control of current in a semiconductor: from the multiphoton to the tunneling regime," Optica **3**, 1358–1361 (2016).
16. S. Sederberg, D. Zimin, S. Keiber, *et al.*, "Attosecond optoelectronic field measurement in solids," Nat. Commun. **11**, 430 (2020).
17. F. Walz, S. Pandey, L. Z. Tan, *et al.*, "Electric field measurement of femtosecond time-resolved four-wave mixing signals in molecules," Opt. Express **30**, 36065–36072 (2022).
18. J. A. Shirley, R. J. Hall, and A. C. Eckbreth, "Folded boxcars for rotational Raman studies," Opt. Lett. **5**, 380–382 (1980).
19. J. Wahlstrand, J. Odhner, E. McCole, *et al.*, "Effect of two-beam coupling in strong-field optical pump-probe experiments," Phys. Rev. A **87**, 053801 (2013).
20. Y.-H. Chen, S. Varma, A. York, *et al.*, "Single-shot, space-and time-resolved measurement of rotational wavepacket revivals in H_2, D_2, N_2, O_2, and N_2O," Opt. Express **15**, 11341–11357 (2007).
21. H. Stapelfeldt and T. Seideman, "Colloquium: aligning molecules with strong laser pulses," Rev. Mod. Phys. **75**, 543 (2003).
22. F. Rosca-Pruna and M. Vrakking, "Experimental observation of revival structures in picosecond laser-induced alignment of I_2," Phys. Rev. Lett. **87**, 153902 (2001).
23. V. Renard, M. Renard, A. Rouzée, *et al.*, "Nonintrusive monitoring and quantitative analysis of strong laser-field-induced impulsive alignment," Phys. Rev. A **70**, 033420 (2004).
24. V. Renard, M. Renard, S. Guérin, *et al.*, "Postpulse molecular alignment measured by a weak field polarization technique," Phys. Rev. Lett. **90**, 153601 (2003).
25. D. N. Fittinghoff, J. L. Bowie, J. N. Sweetser, *et al.*, "Measurement of the intensity and phase of ultraweak, ultrashort laser pulses," Opt. Lett. **21**, 884–886 (1996).
26. B. Lavorel, P. Babilotte, G. Karras, *et al.*, "Measurement of dichroism in aligned molecules," Phys. Rev. A **94**, 043422 (2016).
27. R. Bartels, T. Weinacht, N. Wagner, *et al.*, "Phase modulation of ultrashort light pulses using molecular rotational wave packets," Phys. Rev. Lett. **88**, 013903 (2001).
28. S. M. Gallagher, A. W. Albrecht, J. D. Hybl, *et al.*, "Heterodyne detection of the complete electric field of femtosecond four-wave mixing signals," J. Opt. Soc. Am. B **15**, 2338–2345 (1998).
29. M. A. Hershberger, A. M. Moran, and N. F. Scherer, "New insights into response functions of liquids by electric field-resolved polarization emission time measurements," J. Phys. Chem. B **115**, 5617–5624 (2011).
30. X. Ren, V. Makhija, A.-T. Le, *et al.*, "Measuring the angle-dependent photoionization cross section of nitrogen using high-harmonic generation," Phys. Rev. A **88**, 043421 (2013).
31. V. Makhija, X. Ren, D. Gockel, *et al.*, "Orientation resolution through rotational coherence spectroscopy," arXiv, arXiv:1611.06476 (2016).
32. X. Wang, A.-T. Le, Z. Zhou, *et al.*, "Theory of retrieving orientation-resolved molecular information using time-domain rotational coherence spectroscopy," Phys. Rev. A **96**, 023424 (2017).
33. V. Makhija, J. Tross, V. Kumarappan, *et al.*, "High-order harmonic field retrieval in ethylene," in *EPJ Web of Conferences* (EDP Sciences, 2019), Vol. **205**, paper 02005.
34. P. Sándor, A. Sissay, F. Mauger, *et al.*, "Angle dependence of strong-field single and double ionization of carbonyl sulfide," Phys. Rev. A **98**, 043425 (2018).
35. P. Sándor, A. Sissay, F. Mauger, *et al.*, "Angle-dependent strong-field ionization of halomethanes," J. Chem. Phys. **151**, 194308 (2019).
36. H. V. S. Lam, S. Yarlagadda, A. Venkatachalam, *et al.*, "Angle-dependent strong-field ionization and fragmentation of carbon dioxide measured using rotational wave packets," Phys. Rev. A **102**, 043119 (2020).
37. S. Ramakrishna and T. Seideman, "Dissipative dynamics of laser induced nonadiabatic molecular alignment," J. Chem. Phys. **124**, 034101 (2006).
38. I. V. Litvinyuk, K. F. Lee, P. W. Dooley, *et al.*, "Alignment-dependent strong field ionization of molecules," Phys. Rev. Lett. **90**, 233003 (2003).
39. C. Lin and X. Tong, "Dependence of tunneling ionization and harmonic generation on the structure of molecules by short intense laser pulses," J. Photochem. Photobiol. A **182**, 213–219 (2006).
40. D. Pavičić, K. F. Lee, D. M. Rayner, *et al.*, "Direct measurement of the angular dependence of ionization for N_2, O_2, and CO_2 in intense laser fields," Phys. Rev. Lett. **98**, 243001 (2007).
41. I. Thomann, R. Lock, V. Sharma, *et al.*, "Direct measurement of the angular dependence of the single-photon ionization of aligned N_2 and CO_2," J. Phys. Chem. A **112**, 9382–9386 (2008).
42. C. Marceau, V. Makhija, D. Platzer, *et al.*, "Molecular frame reconstruction using time-domain photoionization interferometry," Phys. Rev. Lett. **119**, 083401 (2017).
43. C. Vozzi, F. Calegari, E. Benedetti, *et al.*, "Controlling two-center interference in molecular high harmonic generation," Phys. Rev. Lett. **95**, 153902 (2005).
44. C. Vozzi, F. Calegari, E. Benedetti, *et al.*, "Probing two-centre interference in molecular high harmonic generation," J. Phys. B **39**, S457 (2006).
45. S. Haessler, J. Caillat, W. Boutu, *et al.*, "Attosecond imaging of molecular electronic wavepackets," Nat. Phys. **6**, 200–206 (2010).
46. J. Itatani, J. Levesque, D. Zeidler, *et al.*, "Tomographic imaging of molecular orbitals," Nature **432**, 867–871 (2004).
47. C. Vozzi, M. Negro, F. Calegari, *et al.*, "Generalized molecular orbital tomography," Nat. Phys. **7**, 822–826 (2011).
48. K. Aidas, C. Angeli, K. L. Bak, *et al.*, "The Dalton quantum chemistry program system," Wires Comput. Mol. Sci. **4**, 269–284 (2014).
49. L. Z. Tan, "UTPS, a computational spectroscopy program," GitLab, 2023, https://gitlab.com/mf-photophysics/utps.
50. A. Srivastava, A. Herbst, M. M. Bidhendi, *et al.*, "Near-petahertz fieldoscopy of liquid," arXiv, arXiv:2310.20512 (2023).